Research article JHEP|Reports

Prevention of lipid droplet accumulation by DGAT1 inhibition ameliorates sepsis-induced liver injury and inflammation

Authors

Lívia Teixeira, Filipe S. Pereira-Dutra, Patrícia A. Reis, Tamires Cunha-Fernandes, Marcos Y. Yoshinaga, Luciana Souza-Moreira, Ellen K. Souza, Ester A. Barreto, Thiago P. Silva, Hugo Espinheira-Silva, Tathiany Igreja, Maísa M. Antunes, Ana Cristina S. Bombaça, Cassiano F. Gonçalves-de-Albuquerque, Gustavo B. Menezes, Eugênio D. Hottz, Rubem F.S. Menna-Barreto, Clarissa M. Maya-Monteiro, Fernando A. Bozza, Sayuri Miyamoto, Rossana C.N. Melo, Patrícia T. Bozza

Correspondence

pbozza@ioc.fiocruz.br, pbozza@gmail.com (P.T. Bozza).

Graphical abstract

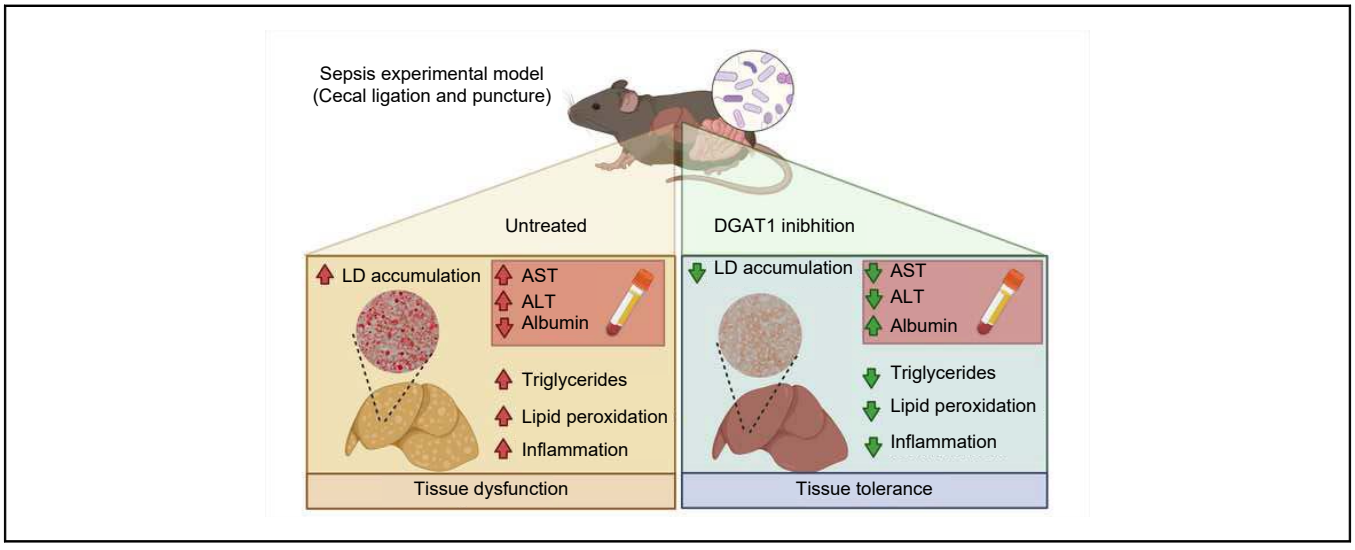

Highlights

- Dysregulated lipid metabolism is a key factor in the hepatic pathology of sepsis.
- Liver LD overload correlates with increased sepsis severity and liver injury.
- Sepsis-induced LDs contain increased levels of unsaturated neutral lipids and lipoperoxides.
- Dampening synthesis of hepatic LDs by inhibiting DGAT1 decreases inflammation, reduces lipid peroxidation, and improves liver function.

Impact and Implications

Sepsis is a complex life-threatening syndrome caused by dysregulated inflammatory and metabolic host responses to infection. The observation that lipid droplets may contribute to sepsis-associated organ injury by amplifying lipid peroxidation and inflammation provides a rationale for therapeutically targeting lipid droplets and lipid metabolism in sepsis.

https://doi.org/10.1016/j.jhepr.2023.100984

Research article

JHEP|Reports

Prevention of lipid droplet accumulation by DGAT1 inhibition ameliorates sepsis-induced liver injury and inflammation

Lívia Teixeira,[1] Filipe S. Pereira-Dutra,[1,2] Patrícia A. Reis,[1,3] Tamires Cunha-Fernandes,[1,2] Marcos Y. Yoshinaga,[4] Luciana Souza-Moreira,[1] Ellen K. Souza,[1] Ester A. Barreto,[1] Thiago P. Silva,[5] Hugo Espinheira-Silva,[1,2] Tathiany Igreja,[1] Maísa M. Antunes,[6] Ana Cristina S. Bombaça,[7,8] Cassiano F. Gonçalves-de-Albuquerque,[1,9] Gustavo B. Menezes,[6] Eugênio D. Hottz,[10] Rubem F.S. Menna-Barreto,[7] Clarissa M. Maya-Monteiro,[1,2] Fernando A. Bozza,[2,11,12] Sayuri Miyamoto,[4] Rossana C.N. Melo,[5] Patrícia T. Bozza[1,2,*]

[1]Laboratory of Immunopharmacology, Oswaldo Cruz Institute, FIOCRUZ, Rio de Janeiro, Brazil; [2]Center for Research, Innovation and surveillance in COVID-19 and Heath Emergencies, FIOCRUZ, Rio de Janeiro, Brazil; [3]Biochemistry Department, Roberto Alcântara Gomes Biology Institute, State University of Rio de Janeiro, Rio de Janeiro, Brazil; [4]Laboratory of Modified Lipids, Department of Biochemistry, University of São Paulo, São Paulo, Brazil; [5]Laboratory of Cellular Biology, Department of Biology, Institute of Biological Sciences (ICB), Federal University of Juiz de Fora, Juiz de Fora, Brazil; [6]Center for Gastrointestinal Biology, Department of Morphology, Institute of Biological Sciences, Federal University of Minas Gerais, Belo Horizonte, Brazil; [7]Laboratory of Cellular Biology, Oswaldo Cruz Institute, FIOCRUZ, Rio de Janeiro, Brazil; [8]Laboratory of Parasitic Disease, Oswaldo Cruz Institute, FIOCRUZ, Rio de Janeiro, Brazil; [9]Laboratory of Immunopharmacology, Department of Physiology, Federal University of the State of Rio de Janeiro, Rio de Janeiro, Brazil; [10]Laboratory of Immunothrombosis, Department of Biochemistry, Federal University of Juiz de Fora (UFJF), Juiz de Fora, Minas Gerais, Brazil; [11]Intensive Care Medicine Laboratory, INI, FIOCRUZ, Rio de Janeiro, Brazil; [12]D'Or Institute Research and Education (IDOr), Rio de Janeiro, Brazil.

JHEP Reports **2024.** https://doi.org/10.1016/j.jhepr.2023.100984

Background & Aims: Lipid droplet (LD) accumulation in cells and tissues is understood to be an evolutionarily conserved tissue tolerance mechanism to prevent lipotoxicity caused by excess lipids; however, the presence of excess LDs has been associated with numerous diseases. Sepsis triggers the reprogramming of lipid metabolism and LD accumulation in cells and tissues, including the liver. The functions and consequences of sepsis-triggered liver LD accumulation are not well known.
Methods: Experimental sepsis was induced by CLP (caecal ligation and puncture) in mice. Markers of hepatic steatosis, liver injury, hepatic oxidative stress, and inflammation were analysed using a combination of functional, imaging, lipidomic, protein expression and immune-enzymatic assays. To prevent LD formation, mice were treated orally with A922500, a pharmacological inhibitor of DGAT1.
Results: We identified that liver LD overload correlates with liver injury and sepsis severity. Moreover, the progression of steatosis from 24 h to 48 h post-CLP occurs in parallel with increased cytokine expression, inflammatory cell recruitment and oxidative stress. Lipidomic analysis of purified LDs demonstrated that sepsis leads LDs to harbour increased amounts of unsaturated fatty acids, mostly 18:1 and 18:2. An increased content of lipoperoxides within LDs was also observed. Conversely, the impairment of LD formation by inhibition of the DGAT1 enzyme reduces levels of hepatic inflammation and lipid peroxidation markers and ameliorates sepsis-induced liver injury.
Conclusions: Our results indicate that sepsis triggers lipid metabolism alterations that culminate in increased liver LD accumulation. Increased LDs are associated with disease severity and liver injury. Moreover, inhibition of LD accumulation decreased the production of inflammatory mediators and lipid peroxidation while improving tissue function, suggesting that LDs contribute to the pathogenesis of liver injury triggered by sepsis.
Impact and Implications: Sepsis is a complex life-threatening syndrome caused by dysregulated inflammatory and metabolic host responses to infection. The observation that lipid droplets may contribute to sepsis-associated organ injury by amplifying lipid peroxidation and inflammation provides a rationale for therapeutically targeting lipid droplets and lipid metabolism in sepsis.

Introduction

Sepsis is a life-threatening multiorgan dysfunction caused by a dysregulated host response to infection[1] that affects approximately 30 million individuals globally annually and remains the leading cause of intensive care unit mortality.[2,3] Multiple organ dysfunction during sepsis is directly linked to morbidity and mortality[1,3] triggered by multifactorial mechanisms, including maladaptive inflammation and disrupted tissue tolerance, which contribute to tissue damage and death.[4,5] Recent studies have emphasised that sepsis-induced

Keywords: immunometabolism; inflammation; sepsis; MODS; steatosis; lipid peroxidation.
Received 28 February 2023; received in revised form 11 November 2023; accepted 21 November 2023; available online 11 December 2023
* Corresponding author. Address: Laboratório de Imunofarmacologia, Instituto Oswaldo Cruz, Fundação Oswaldo Cruz, Avenida Brasil, 4365, Manguinhos, Rio de Janeiro, RJ, CEP 21045–900, Brazil.
E-mail addresses: pbozza@ioc.fiocruz.br, pbozza@gmail.com (P.T. Bozza).

organ dysfunction is associated with substantial alterations in organismal and cellular metabolism. Integrated metabolomics and proteomics analyses have identified lipid metabolism as the primary metabolic alteration that predicts poor outcomes in patients with sepsis compared to healthy individuals.[6,7]

Lipid droplet (LD) accumulation and oxidative stress are recurrent consequences of sepsis-induced metabolic reprogramming.[8] In this way, the liver is under intense overload since it is the central organ in controlling lipid homeostasis.[9] Liver injury is an early outcome of sepsis often detected in the first 24 h after disease onset that occurs concurrently with systemic metabolic remodelling.[10,11] Hepatic steatosis is a commonly observed phenotype in several hepatic injuries, including HCV infection, NAFLD (non-alcoholic fatty liver disease) and NASH (non-alcoholic steatohepatitis).[12,13] Moreover, NAFLD progression to NASH is characterized by the presence of oxidative stress and hepatic inflammatory processes, which contribute to liver failure.[13] However, the role played by LDs in lipotoxic events that are mediated by peroxidised lipids is still controversial.[14,15] Although sepsis induces alterations in lipid metabolism and increased LD accumulation, the involvement of LDs in the mechanisms underlying disrupted tissue tolerance and organ injury in sepsis are poorly understood. Here, we investigated the mechanisms underlying LD formation and its consequences in the liver during sepsis.

Materials and methods

Animals, sepsis induction and treatments

Female C57BL/6J mice were supplied by the Oswaldo Cruz Foundation's Central Animal House and used at 8–12 weeks of age. Mice were maintained on a standard rodent diet (AIN-93 M) with *ad libitum* access to water under a 12-h light/dark cycle and controlled temperature (23 ± 1 °C). Sepsis was induced by caecal ligation and puncture (CLP) according to Reis *et al.* (2017).[16] The number of punctures performed was varied according to the degree of severity sought, with either two perforations (moderate sepsis) or nine perforations (severe sepsis) made using a 22-gauge needle. Sham-operated animals underwent identical laparotomy but without ligation and punctures. At 6 h and 24 h postsurgery, sham and CLP mice were orally treated with 3 mg/kg A922500. Animals were monitored for 48 h for survival, clinical score, and body temperature analysis. The clinical evaluation was based on a multifactorial SHIRPA protocol, with the modifications made by Reis *et al.* (2017).[16] All experiments were approved by the Animal Welfare Committee of the Oswaldo Cruz Foundation under licence numbers LW32/12 and L005/2020 (CEUA/FIOCRUZ).

Intravital confocal microscopy, histology and transmission electron microscopy analysis

Intravital confocal imaging was performed as previously described.[17,18] For histological analysis, the tissue slices were stained with H&E and scanned for analysis using the Panoramic Viewer programme (3DHISTECH Ltd., Budapest, Hungary). For transmission electron microscopy, the samples were fixed in PBS containing 1% osmium tetroxide and 1.5% potassium ferricyanide. The samples were analysed under a transmission electron microscope (EMI, Zeiss). For details, see the supplementary CTAT table.

Mitochondrial respiration

Mitochondrial respiration (O_2 flux) was measured in mouse liver samples using an Oxygraph-2k (Oroboros Instruments, Innsbruck, Austria) as described by Cantó & Garcia-Roves (2015).[19]

Western blotting and dot plot

The livers of mice were harvested using ice-cold lysis buffer pH 8.0 (1% Triton X-100, 2% SDS, 150 mM NaCl, 10 mM HEPES, 2 mM EDTA containing protease inhibitor cocktail; Roche). Western blot analyses were conducted according to the method described by Teixeira *et al.* (2022).[20] The dot plot assay was conducted using 5 μg of liver homogenate protein applied to the blotting apparatus (Bio-Rad) according to the manufacturer's instructions. The densitometry values were analysed using Image Studio Lite software.

Purification of hepatic LD

The livers of the mice were extracted and homogenised in a Dounce tissue grinder at a ratio of 1 g tissue to 3 ml homogenisation buffer (25 mM Tris-HCl, pH 7.5, 100 mM KCl, 1 mM EDTA, 5 mM EGTA) supplemented with antioxidant (BHT, 0.1%), protease and phosphatase inhibitor cocktail (Roche). Hepatic LDs were purified by fractionation in sucrose density gradients according to the method described by Bosh *et al.* (2020).[21] As a control for proper cell fractionation, the activity of the cytoplasmic enzyme lactate dehydrogenase (Promega, G1780) and levels of the LD protein marker PLIN2 were analysed.

Measurement of total glyceride and 8-isoprostane levels in isolated LDs

Total glyceride levels and 8-isoprostane levels in isolated LDs were measured using an enzymatic glyceride liquiform kit (Labtest, cat. # 87-2/100) and enzyme-linked immunoassay (Cayman Chemical, Cat. # 516351), respectively, according to the manufacturer's instructions.

Lipid extraction, lipidomic analysis and data processing

For lipid extraction, we combined 800 μl of methanol with 200 μl of purified LD. Subsequently, 4 ml of chloroform:ethyl acetate (4:1) was added and thoroughly vortexed for 1 min and sonicated for 20 min. After centrifugation (2,000 × *g* for 6 min at 4 °C), the lower phase containing the total lipid extract (TLE) was collected and dried under N_2 gas. The dried TLE was redissolved in 100 μl of isopropanol, and the injection volume was set at 1 μl. We analysed the TLE using an electrospray ionisation time-of-flight mass spectrometer (ESI-TOFMS, Triple TOF 6600, Sciex) interfaced with an ultra-high performance LC system (UHPLC Nexera, Shimadzu). For detailed conditions, please refer to Chaves-Filho *et al.* (2019),[22] the supplementary CTAT table, and Table S1.

Thin-layer chromatography

Hepatic lipid fractions from 1 mg of tissue sample were extracted by applying the Bligh and Dyer method.[23] Thin-layer chromatography was performed on silica gel 60 plates (Merck) according to Horwitz and Perlman (1987).[24]

Thiobarbituric acid-reactive species assay, myeloperoxidase activity and measurements of inflammatory mediators

Thiobarbituric acid-reactive species levels were determined according to the method described by Buege and Aust (1978).[25] Myeloperoxidase activity was analysed using the method described by Bradley *et al.* (1982).[26] CXCL1/KC, CCL2/MCP-1, IFN-γ, IL-1β, IL-6, IL-10, and TNF levels were quantified in liver homogenates by ELISA following the manufacturer's instructions (R&D Systems). The protein concentrations were measured with a BCA protein assay kit.

Statistical analysis

Statistical analyses were performed using GraphPad Prism software version 8. One-way ANOVA followed by Tukey's *post hoc* test was used to compare differences among three groups. Logistic regression was used to analyse the association between lipid droplet amounts and hepatic injury biomarkers. For lipidomic statistical analysis, the data were imported into MetaboAnalyst software (version 5.0; https://www.metaboanalyst.ca/) following the protocol of Pang *et al.*[27] All p values <0.05 were considered statistically significant.

Results

LD accumulation in the hepatic tissue during experimental sepsis occurred alongside liver injury

To evaluate the association between LD accumulation and liver injury, we performed experimental sepsis in mice. Sepsis severity was modulated through the number of punctures made in the caecum. The accumulation of hepatic LDs was higher in the severe sepsis model (9 punctures), with an increased number (Fig. 1B) and droplet size (Fig. 1C), than in the mild model (2 punctures) (Fig. 1A-C). To characterize whether LDs are potential pathophysiological contributors to liver injury during sepsis, we evaluated levels of classic biomarkers of hepatic damage and function, serum alanine aminotransferase (ALT), aspartate aminotransferase (AST) and albumin. The levels of these markers demonstrated the presence of hepatic injury in the sepsis model, although no differences based on severity were observed (Fig. 1D-F). Using logistic regression, we found that the quantity of LDs in the liver was statistically correlated with AST (Fig. 1G), ALT (Fig. 1H) and albumin levels (Fig. 1I). Thus, our results show that LD accumulation is associated with the severity of sepsis and correlates with the degree of sepsis-induced liver injury.

Sepsis-induced hepatic steatosis is followed by an increase in lipid peroxidation

On histological analysis, we detected a marked progression of steatosis processes from 24 h to 48 h post-CLP, with hepatocytes carrying large intracytoplasmic LDs that displaced the nucleus to the cell periphery (macrovesicular steatosis) (Fig. 2A). Through ultrastructural analysis of hepatic LDs, we confirmed size-related

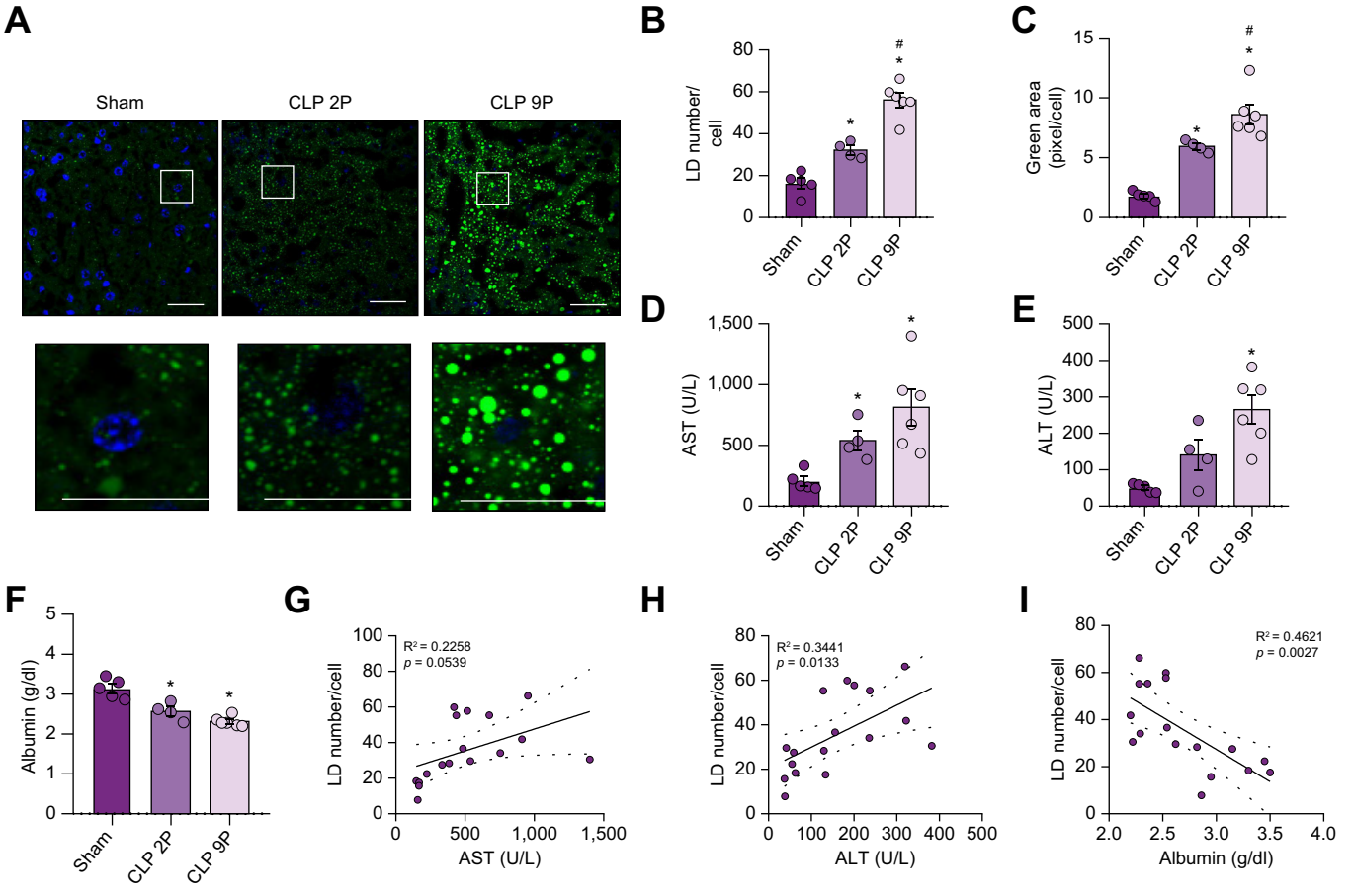

Fig. 1. Hepatic LD accumulation induced by sepsis correlates with hepatic injury. (A) Representative images of BODIPY-labelled LDs (green) in the livers of sham, mild (two punctures) or severe (nine punctures) sepsis mice at 24 h after CLP. Nuclei were visualised by DAPI staining (scale bar: 70 μm). (B–C) Quantification of BODIPY-labelled LDs using ImageJ software. Quantification of LD (B) number and (C) area normalised by the number of cells. Serum levels of (D) AST, (E) ALT, and (F) albumin. Data are expressed as means ± SEM; one-way ANOVA with Tukey's *post hoc* test. *p <0.05 in comparison to the sham group, #p <0.05 in comparison to mild sepsis (two punctures). Experiments were performed with 4-6 mice/group. Logistic regression of (G) AST, (H) ALT, and (I) albumin levels in the serum of mice as a function of LD enumeration 24 h after surgery. ALT, alanine aminotransferase; AST, aspartate aminotransferase; CLP, caecal ligation and puncture; LD, lipid droplet.

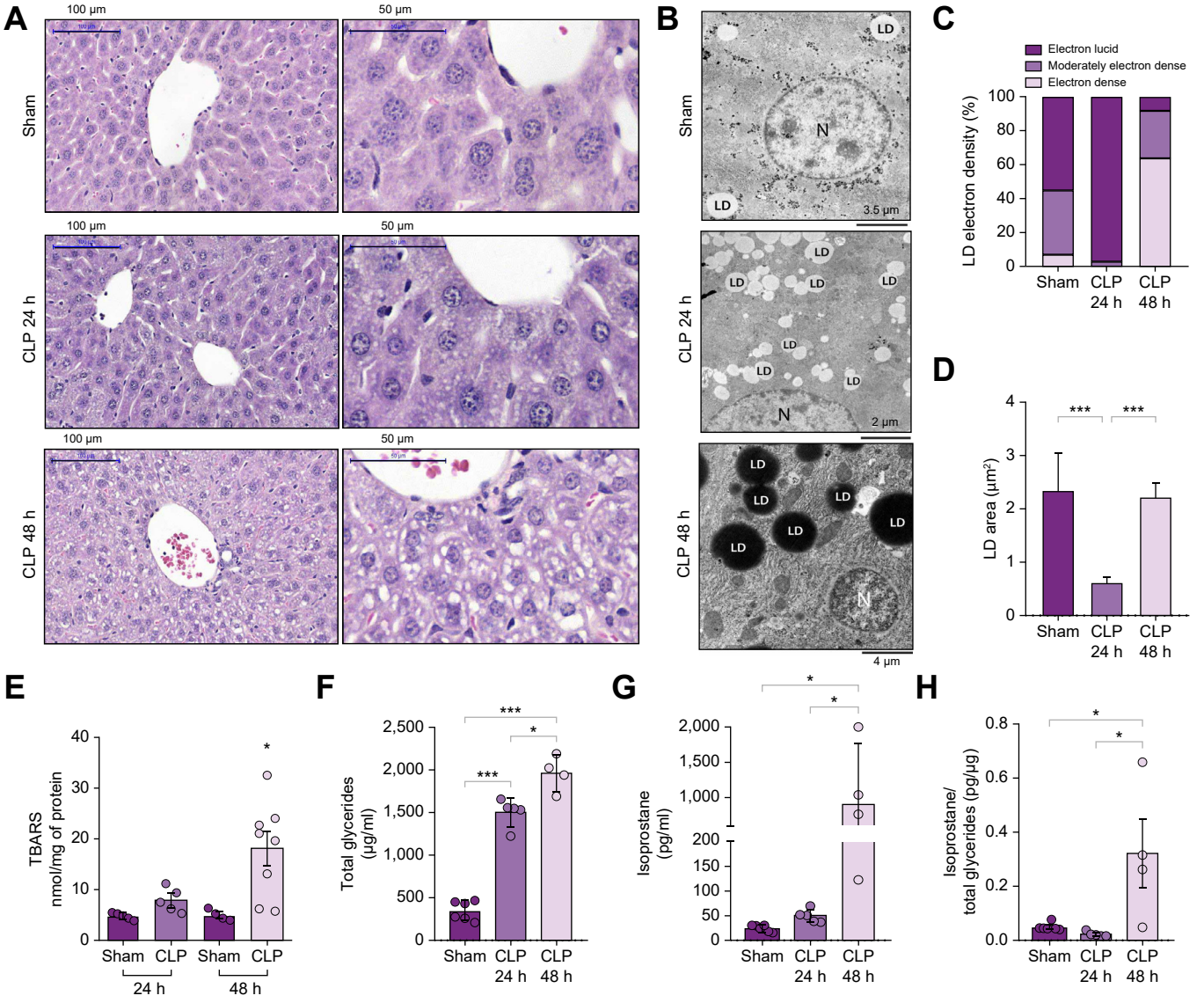

Fig. 2. The progression of hepatic steatosis is followed by an increase in lipid peroxidation over time after sepsis induction. (A) Representative photomicrographs of H&E-stained liver sections from sham and septic mice (mild sepsis – two punctures). (B) Representative electron micrographs of LDs. (C) The percentage of distribution of LDs according to electron density and (C) LD area. A total of 10 electron micrographs and 300 LDs were evaluated. The LDs were classified according to greyscale as electron dense, moderately electron dense and electron lucid (where 0 is absolute black and 255 is absolute white) by using ImageJ software. (D) Concentrations of malondialdehyde in liver homogenates. (E) Total glyceride levels and (F) 8-isoprostane in purified hepatic LDs obtained from the top-to-bottom first fraction of the sucrose gradient. (G) Graph of 8-isoprostane concentration normalised by total glycerides. Experiments were performed with 4-6 mice/group. Data are expressed as means ± SEM; one-way ANOVA with Tukey's *post hoc* test. **p* <0.05. CLP, caecal ligation and puncture; LD, lipid droplet; TBARS, thiobarbituric acid-reactive species.

differences and detected an expressive change in the electron densities of LDs over time during the septic process. At 24 h post-CLP, the LDs were smaller, more numerous, and more electroclear, while at 48 h post-CLP, the LDs were larger and highly electron dense (Fig. 2B-D). Changes in electron density may imply a differential affinity of the cellular components to the metals used in the sample contrasting process, which suggests a change in the composition of the LDs.[28]

Increased levels of end products of lipid peroxidation occur rapidly after sepsis diagnosis and are a strong predictor of severity and mortality.[29] Our next step was to evaluate whether the progression of sepsis-induced liver steatosis was associated with oxidative stress. The evaluation of malondialdehyde (MDA) levels in the total liver homogenate showed that significantly increased lipid peroxidation occurred 48 h after surgery (Fig. 2E). To assess lipid accumulation and peroxidation in the LD content directly, we purified hepatic LDs through sucrose gradient ultracentrifugation and measured the levels of total glycerides along with the level of 8-isoprostane, a prostanoid-like eicosanoid of non-enzymatic origin produced by free radical-catalysed peroxidation of arachidonic acid (AA) and a well-recognised biomarker of lipid peroxidation. Consistent with the extent of hepatic steatosis, we observed a significant increase in liver total glyceride content in the CLP group compared to the sham group at both time points analysed, whereas the total glyceride levels reached a maximum at 48 h (Fig. 2F). Increased lipid peroxidation in LDs, inferred by 8-

isoprostane levels, was also observed only 48 h after the induction of sepsis (Fig. 2G,H). These data suggest that the increase in LD lipid peroxidation results from lipid overload in the liver.

The composition of hepatic LDs changes over time after experimental sepsis induction

Our next step was to assess whether the differences found in the electron density of LDs on electromagnetic analysis were associated with the changes found in LD composition after experimental sepsis. To explore this, untargeted lipidomic analysis was performed in purified hepatic LDs obtained from the first fraction (top-to-bottom) of the sucrose gradient (Fig. 3A). A total of 114 individual lipid species were manually identified by lipidomic analysis. The identified lipids were classified into three subclasses of neutral lipids, mainly triacylglycerols (TGs; n = 109) (Fig. 3B). Moreover, TGs were also the lipid subclass most

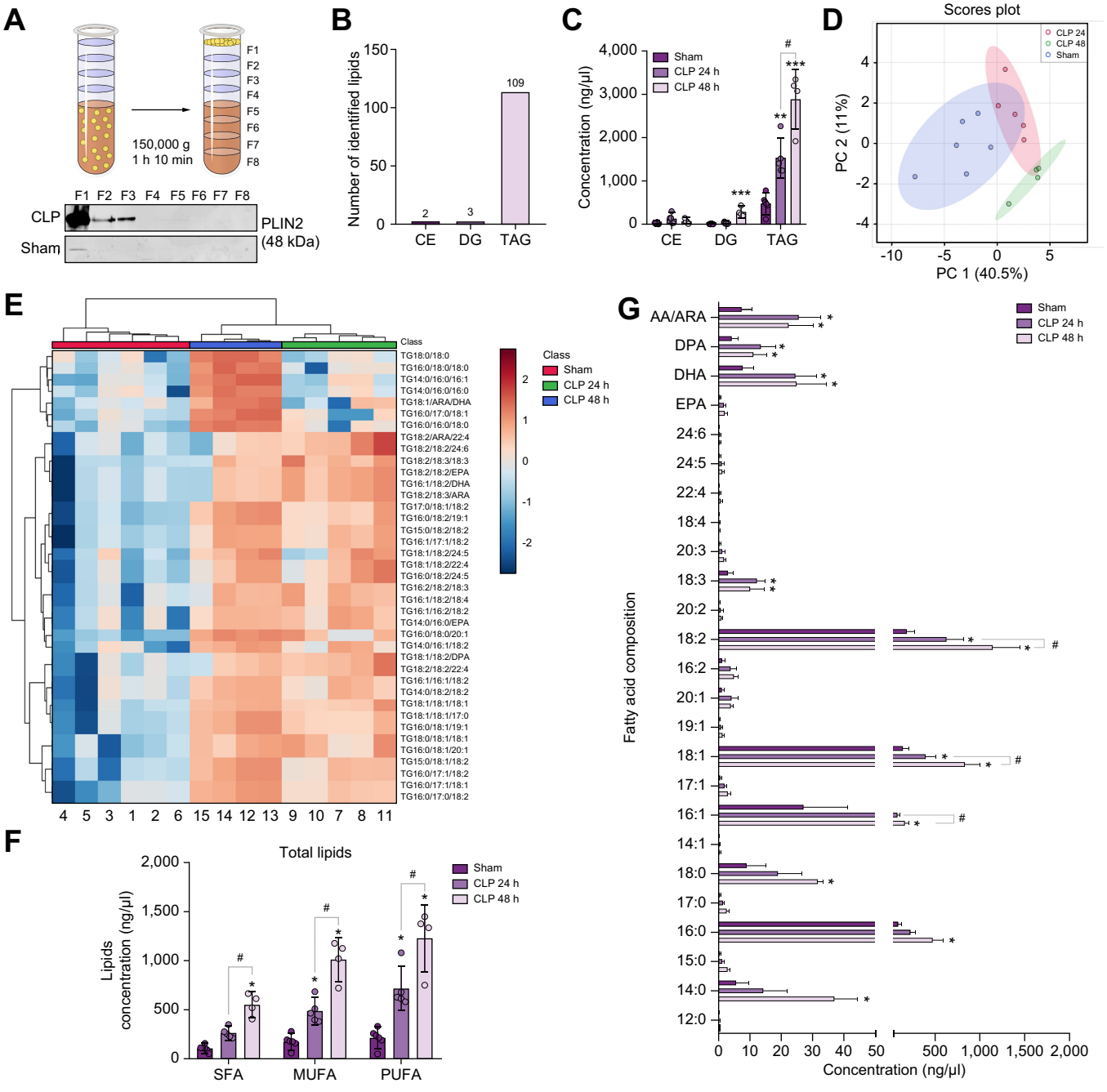

Fig. 3. Sepsis-induced changes in the hepatic LD lipidome profiles of mice. Untargeted lipidomic analysis was performed on the total lipid content of purified hepatic LDs obtained from the top-to-bottom first fraction of the sucrose gradient. (A) Representative diagram of the sucrose gradient, together with Western blotting images showing the presence of LD-structural Plin2 protein from liver sucrose gradients from sham and CLP mice. (B) Number of identified lipid species per lipid subclass. (C) Concentrations of each neutral lipid subclass. (D) Score plot of the principal component analysis. (E) Heatmap displaying sample clusters (n = 4-6 per group) and the top 39 significantly altered lipid species according to ANOVA (p <0.05, FDR-adjusted). (F) The hepatic concentration of total lipids based on the degree of unsaturation and (G) fatty acid composition. AA, arachidonic acid; CE, cholesterol ester; CLP, caecal ligation and puncture; DG, diacylglycerol; DHA, docosahexaenoic acid; DPA, docosapentaenoic acid; EPA, eicosapentaenoic acid; LD, lipid droplet.

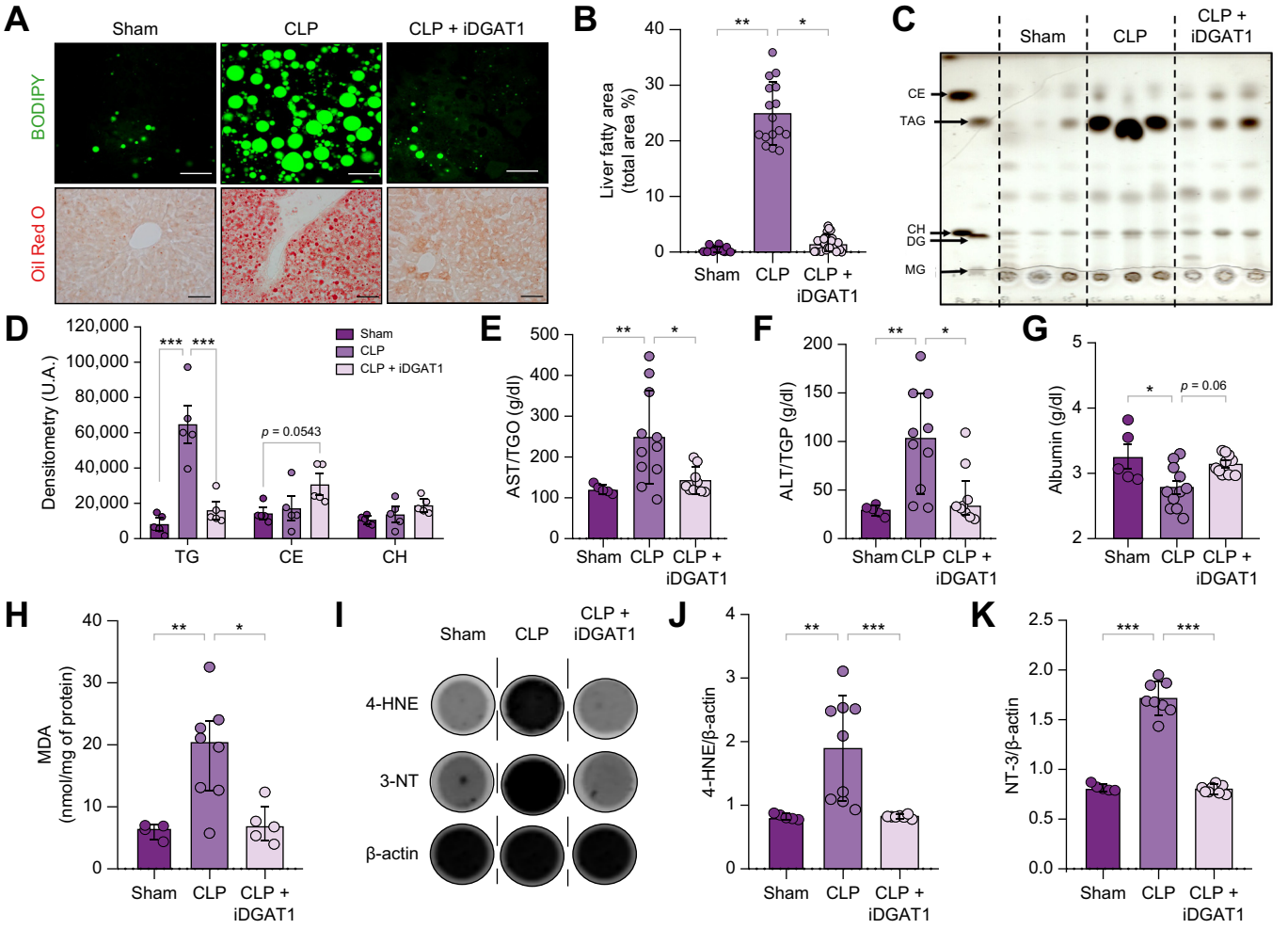

Fig. 4. Inhibition of the DGAT1 enzyme reduces hepatic LD accumulation and lipid peroxidation. Sham or septic mice were orally treated with A922500 (DGAT1 inhibitor, 3 mg/kg) or vehicle and euthanised 48 h after surgery. (A) Intravital confocal microscopy of hepatic LD accumulation (bodipy). Scale bar: 20 μm; and representative micrograph from cryosections of liver tissue stained with Oil Red O (red). Scale bar: 80 μm. (B) Quantitative image quantification of BODIPY fluorescence area per field. of three mouse livers per group. (C) Thin-layer chromatography of liver lipid extract (n = 5 mice/group). Standards: CE, CH, TG, DG and MG. (D) Densitometry from thin-layer chromatography of TG, CE and CH. (E) AST, (F) ALT, and (G) albumin serum levels. (H) Concentrations of MDA in liver homogenates. (I) Representative dot blot of 4-HNE and 3-NT in liver homogenate. β-actin was used as a control for protein loading. (J, K) Dot blot densitometry (Sham n = 5, CLP n = 11, CLP-iDGAT1 n = 9, $^{*}p$ <0.05, $^{**}p$ <0.01, $^{***}p$ <0.001). Data are expressed as means ± SEM; one-way ANOVA with Tukey's *post hoc* test. $^{*}p$ <0.05. 3-NT, 3-nitrotyrosine; 4-HNE, 4-hydroxynonenal; ALT, alanine aminotransferase; AST, aspartate aminotransferase; CE, cholesterol ester; CH, cholesterol; CLP, caecal ligation and puncture; DG, diacylglycerol; DGAT1, diacylglycerol O-acyltransferase 1; iDGAT1, diacylglycerol O-acyltransferase 1 inhibitor; LD, lipid droplet; MDA, malondialdehyde; MG, monoacylglycerol; TG, triacylglycerol.

susceptible to changes induced by sepsis (Fig. 3C). Using principal component analysis, we observed spatial segregation between experimental groups, mainly between the sham and CLP groups at 48 h (Fig. 3D). Based on the degree of unsaturation, sepsis triggered the accumulation of all lipid classes, but mono-unsaturated and polyunsaturated fatty acids (MUFAs and PUFAs, respectively) reached their highest concentrations 48 h after CLP (both increased ∼six-fold compared to the sham group), including eicosapentaenoic acid, docosahexaenoic acid and AA (Fig. 3E). Through a more detailed analysis of the fatty acid composition of TGs, species such as 16:0, 16:1, 18:1 and 18:2 were found in significantly higher concentrations in the LDs of the livers of septic mice after 48 h of CLP, relative to those seen at 24 h (Fig. 3F).

Dampening LD accumulation in septic mice through DGAT1 inhibition protects the liver from lipid peroxidation and tissue damage

Since the main class of neutral lipids accumulated in liver LDs during sepsis was TG, we proceeded to pharmacologically inhibit the diacylglycerol O-acyltransferase 1 (DGAT1) enzyme. We observed that treatment with the DGAT1 inhibitor A922500 (iDGAT1) prevented liver steatosis in septic animals 48 h after CLP surgery (Fig. 4A, B). Thin-layer chromatography analysis confirmed that iDGAT1 treatment reduced TGs, without increasing diacylglycerol accumulation or decreasing cholesterol ester levels in the livers of CLP mice (Fig. 4C, D). The inhibition of LD accumulation in septic mice through DGAT1 blockage reduced AST and ALT levels (Fig. 4E, F) in parallel with the

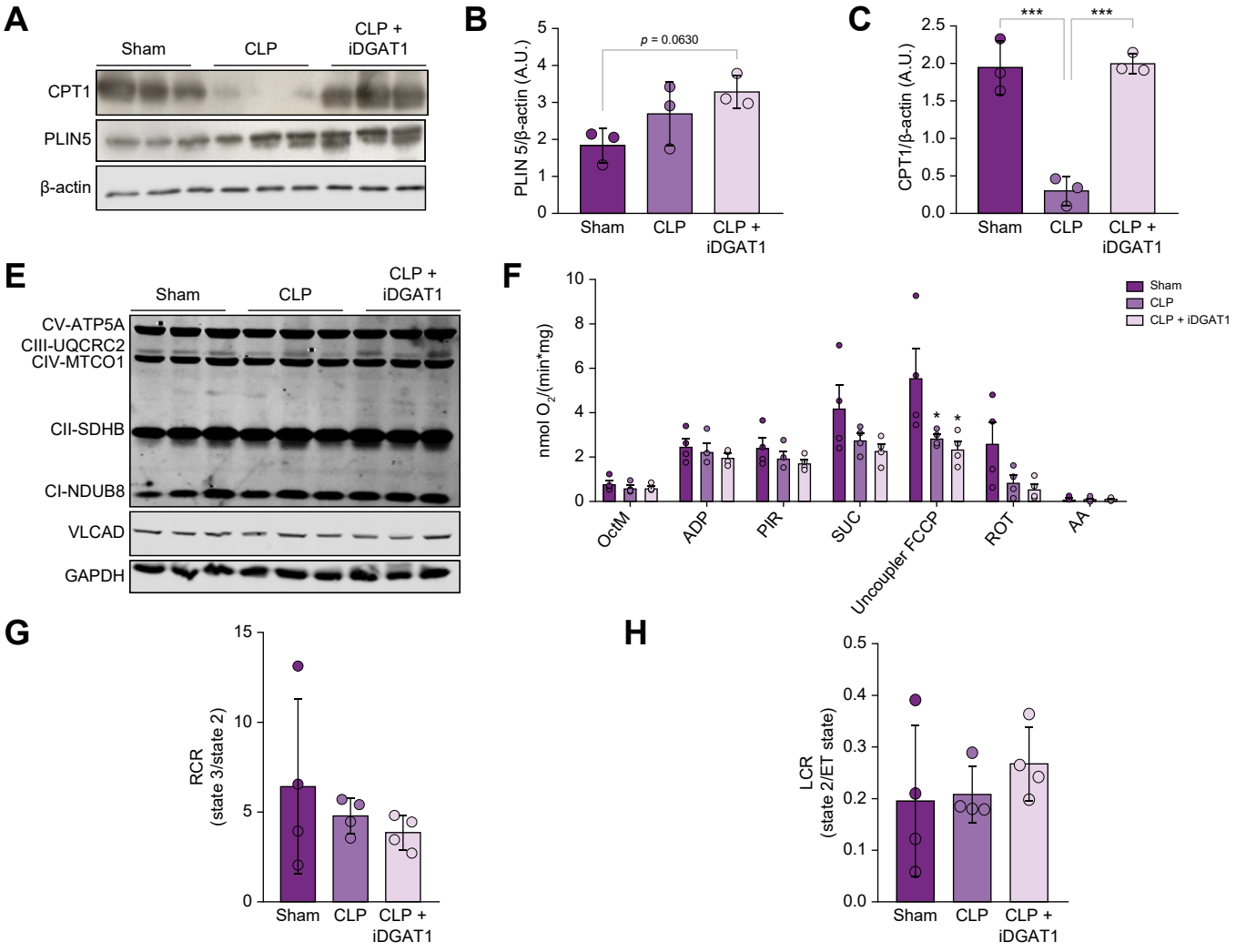

Fig. 5. Inhibition of DGAT1 restored CPT1 expression but did not improve mitochondrial activity. Sham or septic mice were orally treated with A922500 (DGAT1 inhibitor, 3 mg/kg) or vehicle and euthanised 48 h after surgery. (A) Western blotting analysis of CPT1 and PLIN5 in total liver homogenates. β-actin was used as a control for protein loading. Densitometry of (B) PLIN5 and (C) CPT1 expression after loading normalisation. (D) Western blotting analysis of markers of the mitochondrial oxidative phosphorylation system (CV-ATP5A, CIII-UQCRC2, CIV-MTCO1, CII-SDHB and CI-NDUB8) and VLCAD in total liver homogenates. GAPDH was used as a control for protein loading. (E) Mitochondrial respiration (O_2 flux) was measured in mouse liver samples using Oxygraph-2k. (F) The RCR and (G) LCR were calculated using state 3:state 2 and state 2:ET-state ratios. Data are expressed as means ± SEM; one-way ANOVA with Tukey's *post hoc* test. *p <0.05. AA, antimycin A; CLP, caecal ligation and puncture; DGAT1, diacylglycerol O-acyltransferase 1; LCR, leak control ratio; OctM, Octyl L-carnitine; RCR, respiratory control ratio; ROT, rotenone; SUC, succinate.

recovery of albumin production (Fig. 4G). Accordingly, the reduction in LD overload decreased the levels of oxidative stress markers (MDA, 4-hydroxynonenal and 3-nitrotyrosine, Fig. 4H-K) in the liver. For this scenario, one question remained. It was still unknown what the fate of the excess fatty acids would be if they were not channelled to esterification in LDs, as excess free fatty acids also trigger lipotoxicity. As the inhibition of TG formation does not result in the accumulation of precursors, we evaluated the oxidation of fatty acids. Initially, we evaluated the expression of PLIN5, a perilipin protein that regulates LD hydrolysis,[30] and of carnitine palmitoyltransferase 1A (CPT1), a rate-limiting enzyme in fatty acid oxidation. The iDGAT1 treatment caused a trend towards an increase in Plin5 expression compared only to the sham group (Fig. 5A, B). Conversely, treatment with iDGAT1 reestablished the hepatic expression of CPT1, which had been diminished by sepsis (Fig. 5A, C). Once inside the mitochondria, fatty acyl-CoA esters undergo β-oxidation. The oxidation of long-chain fatty acids starts with dehydrogenation catalysed by the VLCAD (also known as ACADVL) enzyme, which is also the rate-limiting step in mitochondrial fatty acid catabolism. No difference in VLCAD expression was observed between the groups (Fig. 5D), suggesting that the impact of DGAT1 inhibition on lipid catabolism relies more on fatty acid transportation to the mitochondria than on β-oxidation itself. We also investigated the expression of proteins associated with the mitochondrial oxidative phosphorylation system (CV-ATP5A, CIII-UQCRC2, CIV-MTCO1, CII-SDHB and CI-NDUB8) (Fig. 5D), and no differences were observed between the experimental groups at 48 h. As previously observed, sepsis triggers mitochondrial respiratory uncoupling; however, DGAT1 inhibition did not modify changes induced by sepsis in respirometry assays using octanoyl-L-carnitine (Fig. 5E, F). Together, these

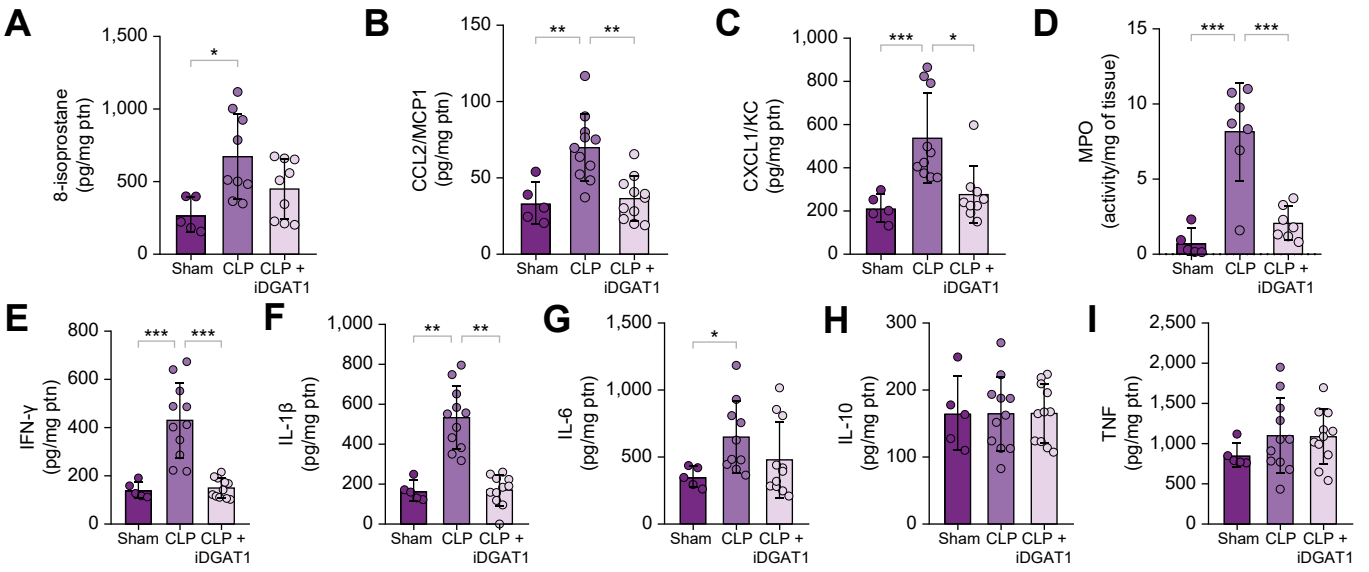

Fig. 6. DGAT1 inhibition reduces proinflammatory responses in the liver tissue of septic mice. Sham or septic mice were orally treated with A922500 (DGAT1 inhibitor, 3 mg/kg) or vehicle and euthanised 48 h after surgery. Liver tissues were homogenised, and the levels of (A) 8-isoprostane were measured by an enzyme-linked immunoassay. The hepatic levels of chemokines (B) CXCL1 and (C) CCL2 were measured by ELISA. (D) MPO activity in liver tissues obtained by an enzymatic assay. The cytokines (E) IFN-γ, (F) IL-1β, (G) IL-6, (H) IL-10 and (I) TNF were measured by ELISA. Data are expressed as means ± SEM; one-way ANOVA with Tukey's *post hoc* test. *p <0.05 (sham n = 5, CLP n = 11, CLP+iDGAT1 n = 9, *p <0.05, **p <0.01, ***p <0.001). CLP, caecal ligation and puncture; iDGAT1, diacylglycerol O-acyltransferase 1 inhibitor.

resus suggest that iDGAT1 treatment has limited direct effects on mitochondrial activity.lt.

Inhibition of DGAT1 decreases liver inflammation but does not improve survival

LDs participate in key mechanisms of the immune response, integrating several immunometabolic signalling pathways, the production of inflammatory mediators, and microbial killing.[31] Since sepsis is fundamentally a disease related to an imbalance in the inflammatory response, we evaluated the effects of pharmacological inhibition of DGAT1 on sepsis-induced liver inflammation. A922500 treatment inhibited sepsis-induced LD formation and 8-isoprostane generation (55% inhibition). Moreover, the treatment also reduced the levels of CCL2/MCP1 (Fig. 6A) and CXCL1/KC (Fig. 6B), chemokines responsible for the recruitment of macrophages and neutrophils. Accordingly, we detected a decrease in myeloperoxidase activity in the livers of iDGAT1-treated mice, indicative of a decrease in leukocyte infiltration of the liver (Fig. 6C). Moreover, treatment with A922500 also significantly reduced the sepsis-induced increases in IFN-γ (Fig. 6D) and IL-1β levels (Fig. 6E) in hepatic tissue. Notably, IL-6, IL-10, and TNF-α levels were not altered by iDGAT1 treatment (Fig. 6F-H). Systemic treatment did not change the sepsis-induced pattern of circulating lipids after 48 h (Fig. 7A-D). However, septic mice treated with iDGAT1 developed persistent hypothermia that probably contributed to their poor outcomes (Fig. 7E). Treatment with iDGAT1 worsened clinical conditions assessed by different markers that composed severity scores (Fig. 7F) and failed to protect mice from mortality at 48 h (Fig. 7G). These data demonstrate that although the inhibition of TG synthesis and LD formation is beneficial for liver preservation, it was not sufficient to protect against sepsis-induced lethality.

Discussion

LD accumulation in non-adipose tissues and oxidative stress are recurrent consequences of sepsis-induced metabolic reprogramming.[32] In this sense, the liver is under intense overload as the central organ in controlling lipid homeostasis.[9] Often detected in the first 24 h after disease onset, liver injury is an early outcome of sepsis that occurs concurrently with systemic metabolic remodelling.[33] Although pronounced alterations in lipid metabolism and LD accumulation are observed during sepsis, their involvement in the mechanisms of disrupted tissue tolerance and organ injury in sepsis is poorly understood. We propose that under an environment of heightened inflammation and oxidative stress, this mechanism of tissue tolerance is disrupted and that LDs contribute to the amplification of lipid peroxidation and inflammation.

The current view places LD accumulation as an evolutionarily conserved mechanism of tolerance to avoid lipid-induced toxicity[34] due to the ability of LDs to buffer excess free fatty acids in stressful situations and release them gradually to meet cellular needs.[35] Herein, we report that the accumulation of LDs in the liver is a feature of the pathophysiology of sepsis and is associated with the severity of sepsis and the increase in levels of markers of liver injury. We also demonstrated that with the progression of hepatic steatosis, LD accumulation could contribute to sepsis-induced inflammation and lipid peroxidation. The increase in end products of lipid peroxidation occurs rapidly after the diagnosis of sepsis and is a strong predictor of severity and mortality.[29] Organs and systems are differentially affected by the overload of peroxidised lipids, and the hepatic system has been shown to be one of the most highly susceptible.[36,37]

In sepsis, tissue damage results from a maladaptative inflammatory and metabolic response mounted to resist infection; this is

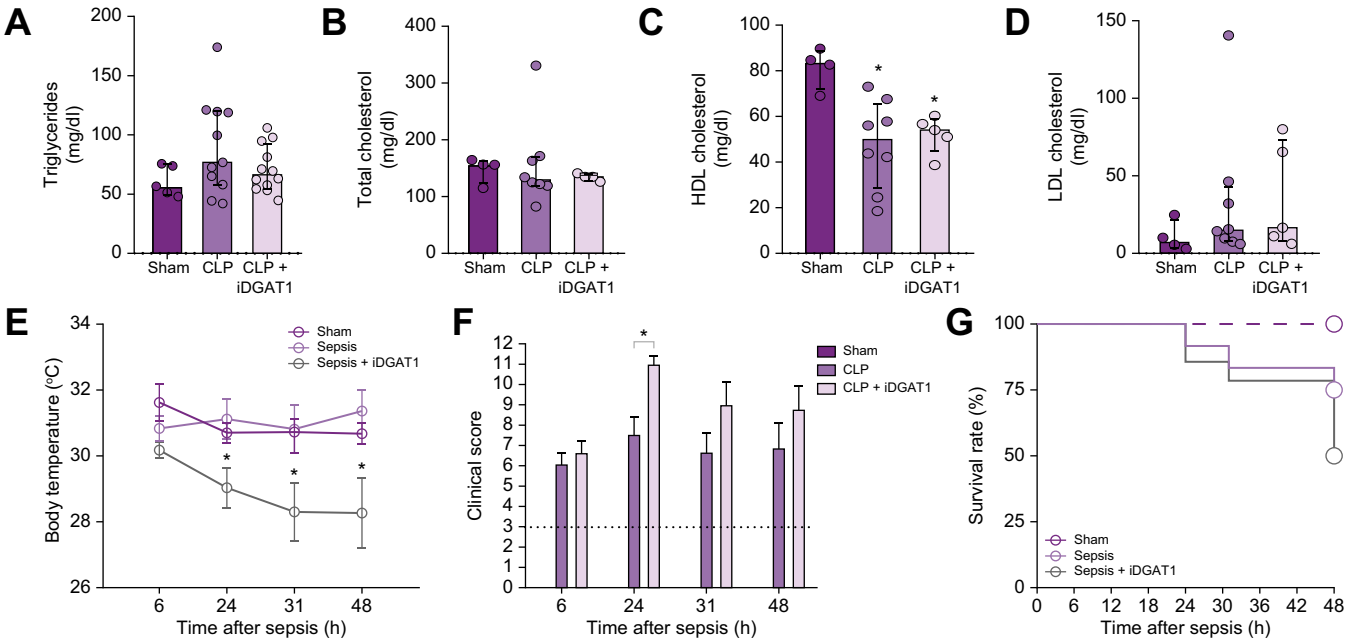

Fig. 7. Inhibition of triglyceride synthesis does not improve the survival rates of septic mice. Sham or septic mice were orally treated with A922500 (DGAT1 inhibitor, 3 mg/kg) or vehicle. Serum lipid concentrations were determined at 48 h post-CLP. (A) Triglycerides, (B) total cholesterol, (C) HDL cholesterol and (D) LDL cholesterol. (E) Graph of body temperature fluctuations after CLP surgery. (F) Clinical score determination of mouse sepsis severity. Experiments were performed with 4-8 mice/group. Data are expressed as means ± SEM; one-way ANOVA with Tukey's *post hoc* test. **p* <0.05. (G) The survival rate was statistically assessed by the log-rank (Mantel–Cox) test. Sham n = 5, CLP n = 11, CLP+iDGAT1 n = 9). CLP, caecal ligation and puncture; iDGAT1, diacylglycerol O-acyltransferase 1 inhibitor.

associated with inadequate mechanisms of tissue tolerance.[38] Moreover, inflammatory activation of the immune system, together with mitochondrial dysfunction, are the most potent sources of reactive species during sepsis,[39] contributing to sepsis-induced lipid peroxidation. We demonstrate that inhibiting hepatic LD accumulation by targeting the enzyme DGAT1 reduces levels of inflammatory mediators and lipid peroxidation while improving liver function in sepsis. Our findings support the well-established role of LDs in inflammatory mediator production, being a site for AA accumulation and a platform for eicosanoid synthesis.[40] In this context, lipidomic analysis of purified LDs showed increased levels of AA during sepsis compared to those seen in sham animals. Moreover, our results show that sepsis-induced LDs are sites of 8-isoprostane generation, a non-enzymatic eicosanoid produced by oxidative stress-induced AA peroxidation, as well as a biomarker of lipid peroxidation. 8-isoprostane is also a proinflammatory mediator[41] involved in the activation and recruitment of neutrophils.[42,43] Conversely, impairment of sepsis-triggered LD biogenesis by DGAT1 inhibition was accompanied by a reduction in 8-isoprostane formation in the liver, decreased myeloperoxidase activity and reduced levels of CXCL1 and CCL2, suggesting a role for LDs in lipid peroxidation, inflammation and leukocyte infiltration in the liver. Moreover, reductions in CXCL1, CCL2, IL-1β, IL-6 and IFN-γ levels have been shown to protect against sepsis-induced multiple organ dysfunction.[44–46]

Oral iDGAT1 treatment completely reversed sepsis-induced hepatic steatosis and reduced tissue MDA levels. However, DGAT1 inhibition did not result in the accumulation of diacylglycerol, a cytotoxic lipid. The absence of TG precursor accumulation following DGAT1 inhibition may be linked to the restoration of CPT1 expression, which facilitates fatty acid transport for β-oxidation. Indeed, the deletion of DGAT1 has been demonstrated to enhance the expression of genes related to fatty acid oxidation while reducing the expression of those associated with adipogenesis.[47]

Despite its protective effect against liver injury, the inhibition of LD accumulation did not protect against sepsis mortality. This result could be associated in part with the increase in basal energy expenditure induced by systemic DGAT1 inhibition, a phenotype also observed in *Dgat1* knockout mice.[48] Given that resisting a systemic infection entails significant energy expenditure, this elevation in basal energy consumption compromises the maintenance of fundamental homeostatic functions, as evidenced by the loss of control over body temperature. Therefore, the exacerbated increase in energy demand in CLP mice treated with iDGAT1 may explain the negative survival outcomes. Future studies will be necessary to better characterize the metabolic regulation by DGAT1 during sepsis.

In conclusion, our results demonstrate that sepsis triggers lipid metabolism reprogramming that culminates with increased LD accumulation in the liver. Increased abundance of LDs is associated with disease severity and liver injury in sepsis. Conversely, blocking LD accumulation through DGAT1 inhibition improved liver function through mechanisms that involve, at least in part, decreased inflammation and lipid peroxidation in the liver. By identifying that LDs may contribute to the pathogenesis of liver injury triggered by sepsis, our observations provide a rationale for therapeutic targeting of LDs and lipid metabolism in sepsis.

Abbreviations

AA, arachidonic acid; CLP, caecal ligation and puncture; CPT1, carnitine palmitoyltransferase 1A; DGAT1, diacylglycerol O-acyltransferase 1; iDGAT1, diacylglycerol O-acyltransferase 1 inhibitor; LDs, lipid droplets; MDA, malondialdehyde; TG, triacylglycerol; TLE, total lipid extract.

Financial support

This work was supported by grants from Conselho Nacional de Desenvolvimento Científico e Tecnológico (CNPq, grant 311686/2019-2), Fundação de Amparo a Pesquisa do Estado do Rio de Janeiro (FAPERJ grant E-26/211.316/2021 and E-26/200.992/2021), Coordenação de Aperfeiçoamento de Pessoal de Nível Superior (CAPES, grant 23038.003950/2020-16) and Human Frontier Science Program (HFSP, grant RGP 0020/2015). SM was supported by Fundação de Amparo à Pesquisa do Estado de São Paulo (FAPESP, CEPID–Redoxoma grant 13/07937-8) and CNPq (grant 313926/2021-2). RCNM was supported by CNPq (grant 307270/2022-0) and Fundação de Amparo à Pesquisa do Estado de Minas Gerais (FAPEMIG, grant APQ-02930-21).

Conflict of interest

The authors declare no competing interests.

Please refer to the accompanying ICMJE disclosure forms for further details.

Authors' contributions

LT and PTB conceptualised the study. LT, FSP-D, PAR, and PTB were responsible for the design and conducted the main experiments. Contributing to the in vivo treatment, CLP surgeries and in vivo data collection: LT, FSP-D, PAR, TF-C, TI and CFG-A. Ex vivo analysis: EKS, LS-M, HE-S, MMA, EDH, CMM-M. Performing respirometry analysis and data processing: ACSB. Performing lipidomic analysis and data processing: LT, EAB, and MYY. RFSM-B, GBM, RFAB, SM, RCNM and PTB contributed to the study design and data analysis and critically revised the article. The manuscript was drafted by LT, FSP-D, and PTB and edited by all authors. All authors contributed to the article and approved the submitted version.

Data availability statement

The data supporting the findings are available upon request to the corresponding author (PTB). Lipidomic data are available in Supplementary table S1. Methods, materials, and resources are included in the Materials and Supplementary CTAT Table.

Acknowledgements

We thank the Fiocruz Luminex Platform (*Subunidade Luminex-RPT03C* Rede de Plataformas PDTIS, FIOCRUZ/RJ) and the assistance of MSc Edson Fernandes de Assis for the use of its Luminex facilities. The authors are grateful to Centro de Microscopia (UFMG/MG) for electron microscopy image acquisition.

Supplementary data

Supplementary data to this article can be found online at https://doi.org/10.1016/j.jhepr.2023.100984.

References

Author names in bold designate shared co-first authorship

[1] Singer M, Deutschman CS, Seymour CW, et al. The third international consensus definitions for sepsis and septic shock (Sepsis-3). JAMA 2016;315:801. https://doi.org/10.1001/jama.2016.0287.

[2] Rudd KE, Johnson SC, Agesa KM, et al. Global, regional, and national sepsis incidence and mortality, 1990–2017: analysis for the Global Burden of Disease Study. Lancet 2020;395:200–211. https://doi.org/10.1016/S0140-6736(19)32989-7.

[3] Fleischmann C, Scherag A, Adhikari NKJ, et al. Assessment of global incidence and mortality of hospital-treated sepsis. Current estimates and limitations. Am J Respir Crit Care Med 2016;193:259–272. https://doi.org/10.1164/rccm.201504-0781°C.

[4] Lelubre C, Vincent J-L. Mechanisms and treatment of organ failure in sepsis. Nat Rev Nephrol 2018;14:417–427. https://doi.org/10.1038/s41581-018-0005-7.

[5] Wang A, Luan HH, Medzhitov R. An evolutionary perspective on immunometabolism. Science (1979) 2019;363:eaar3932. https://doi.org/10.1126/science.aar3932.

[6] Wang A, Huen SC, Luan HH, et al. Opposing effects of fasting metabolism on tissue tolerance in bacterial and viral inflammation. Cell 2016;166:1512–1525.e12. https://doi.org/10.1016/j.cell.2016.07.026.

[7] **Weis S**, **Carlos AR**, **Moita MR**, et al. Metabolic adaptation establishes disease tolerance to sepsis. Cell 2017;169:1263–1275.e14. https://doi.org/10.1016/j.cell.2017.05.031.

[8] **Van Wyngene L**, **Vandewalle J**, **Libert C**. Reprogramming of basic metabolic pathways in microbial sepsis: therapeutic targets at last? EMBO Mol Med 2018;10:e8712. https://doi.org/10.15252/emmm.201708712.

[9] Beyer D, Hoff J, Sommerfeld O, et al. The liver in sepsis: molecular mechanism of liver failure and their potential for clinical translation. Mol Med 2022;28:84. https://doi.org/10.1186/s10020-022-00510-8.

[10] Langley RJ, Tsalik EL, Velkinburgh JCv, et al. An integrated clinico-metabolomic model improves prediction of death in sepsis. Sci Transl Med 2013;5:195ra95. https://doi.org/10.1126/scitranslmed.3005893. 195ra95.

[11] Kramer L, Jordan B, Druml W, et al. Incidence and prognosis of early hepatic dysfunction in critically ill patients - a prospective multicenter study. Crit Care Med 2007. https://doi.org/10.1097/01.CCM.0000259462.97164.A0.

[12] Mashek DG. Hepatic lipid droplets: a balancing act between energy storage and metabolic dysfunction in NAFLD. Mol Metab 2020;50:101115. https://doi.org/10.1016/j.molmet.2020.101115.

[13] Scorletti E, Carr RM. A new perspective on NAFLD: focusing on lipid droplets. J Hepatol 2022;76:934–945. https://doi.org/10.1016/j.jhep.2021.11.009.

[14] Jarc E, Kump A, Malavašič P, et al. Lipid droplets induced by secreted phospholipase A2 and unsaturated fatty acids protect breast cancer cells from nutrient and lipotoxic stress. Biochim Biophys Acta (BBA) Mol Cell Biol Lipids 2018;1863:247–265. https://doi.org/10.1016/j.bbalip.2017.12.006.

[15] Liu L, MacKenzie KR, Putluri N, et al. The Glia-neuron lactate shuttle and elevated ROS promote lipid synthesis in neurons and lipid droplet accumulation in Glia via APOE/D. Cell Metab 2017. https://doi.org/10.1016/j.cmet.2017.08.024.

[16] Reis PA, Alexandre PCB, D'Avila JC, et al. Statins prevent cognitive impairment after sepsis by reverting neuroinflammation, and microcirculatory/endothelial dysfunction. Brain Behav Immun 2017;60:293–303. https://doi.org/10.1016/j.bbi.2016.11.006.

[17] Marques PE, Antunes MM, David BA, et al. Imaging liver biology in vivo using conventional confocal microscopy. Nat Protoc 2015;10:258–268. https://doi.org/10.1038/nprot.2015.006.

[18] Diniz AB, Antunes MM, Lacerda VA, et al. Imaging and immunometabolic phenotyping uncover changes in the hepatic immune response in the early phases of NAFLD. JHEP Rep 2020;2:100117. https://doi.org/10.1016/j.jhepr.2020.100117.

[19] Cantó C, Garcia-Roves PM. High-resolution respirometry for mitochondrial characterization of ex vivo mouse tissues. Curr Protoc Mouse Biol 2015;5:135–153. https://doi.org/10.1002/9780470942390.mo140061.

[20] **Teixeira L**, **Temerozo JR**, **Pereira-Dutra FS**, et al. Simvastatin down-regulates the SARS-CoV-2-induced inflammatory response and impairs viral infection through disruption of lipid rafts. Front Immunol 2022:1–16.

[21] **Bosch M**, **Sánchez-Álvarez M**, **Fajardo A**, et al. Mammalian lipid droplets are innate immune hubs integrating cell metabolism and host defense. Science (1979) 2020;370:eaay8085. https://doi.org/10.1126/science.aay8085.

[22] Chaves-Filho AB, Pinto IFD, Dantas LS, et al. Alterations in lipid metabolism of spinal cord linked to amyotrophic lateral sclerosis. Sci Rep 2019;9:1–14. https://doi.org/10.1038/s41598-019-48059-7.

[23] Bligh EG, Dyer WJ. A rapid method of total lipid extraction and purification. Can J Biochem Physiol 1959;37:911–917. https://doi.org/10.1139/o59-099.

[24] Horwitz J, Perlman RL. Measurement of inositol phospholipid metabolism in PC12 pheochromocytoma cells. Methods Enzymol 1987;141:169–175. https://doi.org/10.1016/0076-6879(87)41065-3.
[25] Buege JA, Aust SD. [30] Microsomal lipid peroxidation. Methods 1978;78:302–310. https://doi.org/10.1016/S0076-6879(78)52032-6.
[26] Bradley PP, Priebat DA, Christensen RD, et al. Measurement of cutaneous inflammation: estimation of neutrophil content with an enzyme marker. J Invest Dermatol 1982;78:206–209. https://doi.org/10.1111/1523-1747.ep12506462.
[27] Pang Z, Zhou G, Ewald J, et al. Using MetaboAnalyst 5.0 for LC–HRMS spectra processing, multiomics integration and covariate adjustment of global metabolomics data. Nat Protoc 2022;17:1735–1761. https://doi.org/10.1038/s41596-022-00710-w.
[28] Cheng J, Fujita A, Ohsaki Y, et al. Quantitative electron microscopy shows uniform incorporation of triglycerides into existing lipid droplets. Histochem Cell Biol 2009:132. https://doi.org/10.1007/s00418-009-0615-z.
[29] Lorente L, Martín MM, Abreu-González P, et al. Sustained high serum malondialdehyde levels are associated with severity and mortality in septic patients. Crit Care 2013. https://doi.org/10.1186/cc13155.
[30] Wang H, Sreenevasan U, Hu H, et al. Perilipin 5, a lipid droplet-associated protein, provides physical and metabolic linkage to mitochondria. J Lipid Res 2011;52:2159–2168. https://doi.org/10.1194/jlr.M017939.
[31] Bosch M, Pol A. Eukaryotic lipid droplets: metabolic hubs, and immune first responders. Trends Endocrinol Metab 2022;33. https://doi.org/10.1016/j.tem.2021.12.006.
[32] Van Wyngene L, Vandewalle J, Libert C. Reprogramming of basic metabolic pathways in microbial sepsis: therapeutic targets at last? EMBO Mol Med 2018;10(8). https://doi.org/10.15252/emmm.201708712.
[33] Langley RJ, Tsalik EL, Velkinburgh JCv, et al. An integrated clinico-metabolomic model improves prediction of death in sepsis. Sci Transl Med 2013;5:195ra95. https://doi.org/10.1126/scitranslmed.3005893. 195ra95.
[34] Bailey AP, Koster G, Guillermier C, et al. Antioxidant role for lipid droplets in a stem cell niche of Drosophila. Cell 2015;163:340–353. https://doi.org/10.1016/j.cell.2015.09.020.
[35] Olzmann JA, Carvalho P. Dynamics and functions of lipid droplets. Nat Rev Mol Cell Biol 2019. https://doi.org/10.1038/s41580-018-0085-z.
[36] Toufekoula C, Papadakis V, Tsaganos T, et al. Compartmentalization of lipid peroxidation in sepsis by multidrug-resistant gram-negative bacteria: experimental and clinical evidence. Crit Care 2013;17(1):R6. https://doi.org/10.1186/cc11930.
[37] Ware LB, Fessel JP, May AK, et al. Plasma biomarkers of oxidant stress and development of organ failure in severe sepsis. Shock 2011;36:12–17. https://doi.org/10.1097/SHK.0b013e318217025a.
[38] Luan HH, Wang A, Hilliard BK, et al. GDF15 is an inflammation-induced central mediator of tissue tolerance. Cell 2019;178:1231–1244.e11. https://doi.org/10.1016/j.cell.2019.07.033.
[39] McBride MA, Owen AM, Stothers CL, et al. The metabolic basis of immune dysfunction following sepsis and trauma. Front Immunol 2020;11. https://doi.org/10.3389/fimmu.2020.01043.
[40] Pereira-Dutra FS, Teixeira L, Souza Costa MF, Bozza PT. Fat, fight, and beyond: the multiple roles of lipid droplets in infections and inflammation. J Leukoc Biol 2019;106:563–580. https://doi.org/10.1002/JLB.4MR0119-035R.
[41] Scholz H, Yndestad A, Damås JK, et al. 8-Isoprostane increases expression of interleukin-8 in human macrophages through activation of mitogen-activated protein kinases. Cardiovasc Res 2003;59:945–954. https://doi.org/10.1016/S0008-6363(03)00538-8.
[42] Fontana L, Giagulli C, Minuz P, et al. 8-Iso-PGF2α induces β2-integrin–mediated rapid adhesion of human polymorphonuclear neutrophils. Arterioscler Thromb Vasc Biol 2001;21:55–60. https://doi.org/10.1161/01.ATV.21.1.55.
[43] Fontana L, Giagulli C, Cominacini L, et al. β2 integrin-dependent neutrophil adhesion induced by minimally modified low-density lipoproteins is mainly mediated by F2-isoprostanes. Circulation 2002;106:2434–2441. https://doi.org/10.1161/01.CIR.0000037223.92135.38.
[44] **Li X**, **Fu H**, **Yi W**, et al. Dual role of leukotriene B4 receptor type 1 in experimental sepsis. J Surg Res 2015;193:902–908. https://doi.org/10.1016/j.jss.2014.09.013.
[45] Kwon S-Y, Ro M, Kim J-H. Mediatory roles of leukotriene B4 receptors in LPS-induced endotoxic shock. Sci Rep 2019;9:5936. https://doi.org/10.1038/s41598-019-42410-8.
[46] Bozza FA, Salluh JI, Japiassu AM, et al. Cytokine profiles as markers of disease severity in sepsis: a multiplex analysis. Crit Care 2007;11. https://doi.org/10.1186/cc5783.
[47] Chen HC, Smith SJ, Ladha Z, et al. Increased insulin and leptin sensitivity in mice lacking acyl CoA:diacylglycerol acyltransferase 1. J Clin Invest 2002;109:1049–1055. https://doi.org/10.1172/jci200214672.
[48] Smith SJ, Cases S, Jensen DR, et al. Obesity resistance and multiple mechanisms of triglyceride synthesis in mice lacking Dgat. Nat Genet 2000;25:87–90. https://doi.org/10.1038/75651.